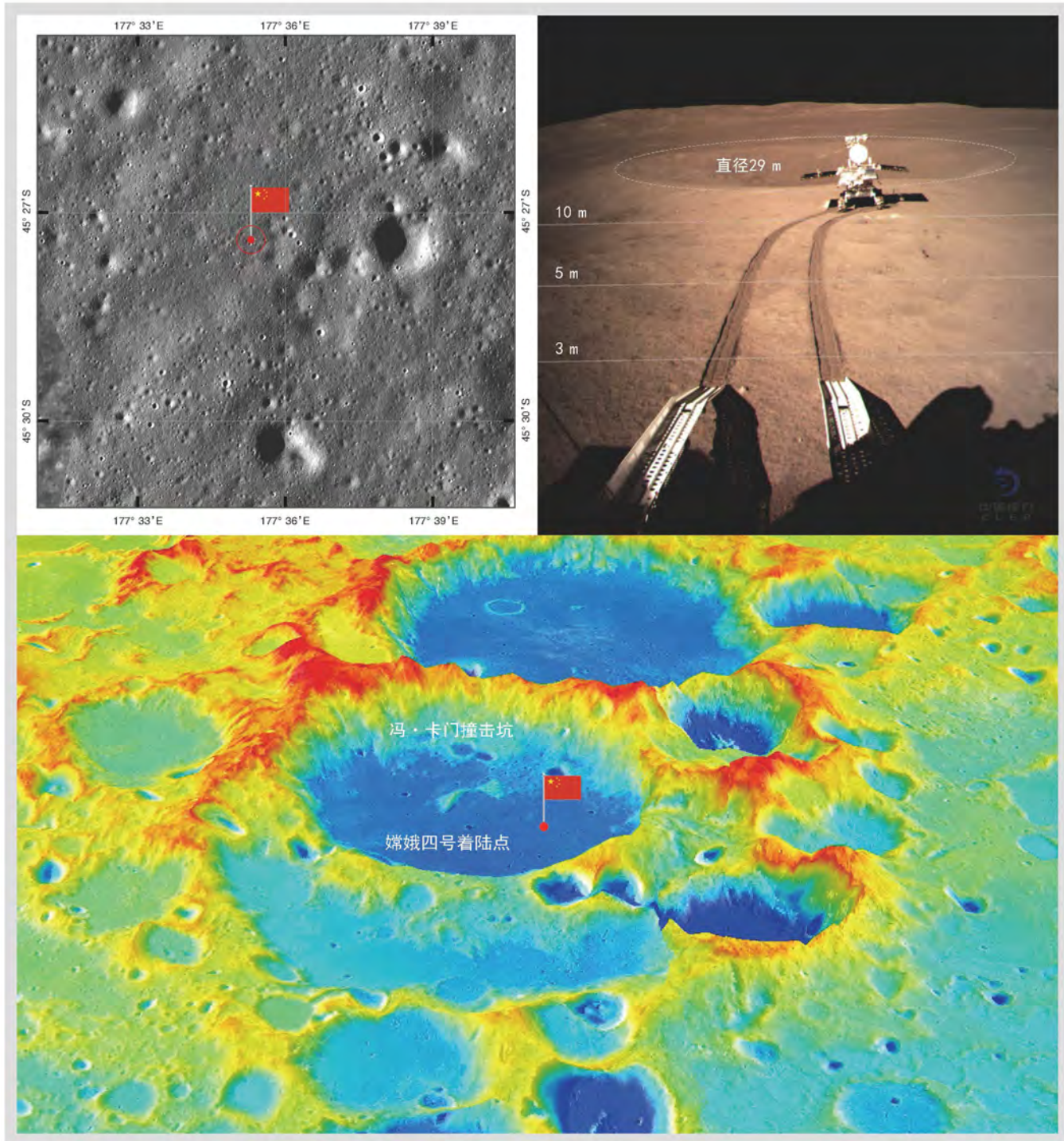


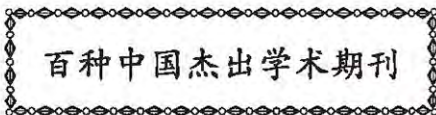
主办
出版
科学出版社
中国地理学会环境遥感分会
中国科学院遥感与数字地球研究所

JOURNAL OF REMOTE SENSING

遥 感 学 报

2019年 Vol.23 第23卷 No.1 第1期 ISSN 1007-4619 CN11-3841 / TP CODEN YXAUAB





遥感学报

Yaogan Xuebao

第 23 卷 第 1 期 2019 年 1 月

目 次

综述

- 发展几何光学遥感建模理论，推动定量遥感科学前行——深切缅怀李小文院士
柳钦火，阎广建，焦子锑，肖青，闻建光，梁顺林，王锦地 (1)

基础理论

- 异质性地表反照率遥感产品真实性检验研究现状及挑战 吴小丹，肖青，闻建光，游冬琴 (11)
地表净辐射通量观测、模拟和同化的研究进展
赵丽芳，沈占锋，李春明，邹丽静，郭明，孙源，彭漫 (24)

- 日光诱导叶绿素荧光遥感反演及碳循环应用进展 章钊颖，王松寒，邱博，宋练，张永光 (37)
机载 WIDAS 数据的 Landsat 卫星反照率初步验证
何丹丹，焦子锑，董亚冬，张小宁，丁安心，尹思阳，崔磊，常雅轩 (53)

- 多模型耦合下的植被冠层可燃物含水率遥感反演 全兴文，何彬彬，刘向苗，廖展芒，邱实，殷长明 (62)
技术方法

- 联合 EEMD-KECA 算法的 InSAR 干涉相位时频滤波
余洁，刘利敏，李小娟，朱琳，谢东海，陈蜜 (78)
全波形激光雷达回波分解方法 李洪鹏，李国元，蔡志坚，吴冠豪 (89)
余弦调相散射波干扰对 SAR 双通道对消干扰抑制的影响 张云鹏，毕大平，周阳，张博，房明星 (99)
偏振激光雷达探测大气—水体光学参数廓线.....

- 周雨迪，刘东，徐沛拓，毛志华，陈鹏，刘志鹏，刘群，唐培钧，张与鹏，王雪霁，任佳炜，金时伟 (108)
空间碎片探测卫星成像 CCD 的在轨辐射效应分析 李豫东，文林，黄建余，文延，张科科，郭旗 (116)
遥感应用

- 高分辨率遥感影像建筑物分级提取 游永发，王思远，王斌，马元旭，申明，刘卫华，肖琳 (125)
广东省和江苏省大气甲醛时空变化对比分析
朱松岩，李小英，程天海，余超，王新辉，苗晶，侯灿 (137)

- 新疆地区鸟类和哺乳动物丰富度与环境因子的空间格局与关系
龙昶宇，万华伟，李利平，王锦地 (155)
决策树结合混合像元分解的中国竹林遥感信息提取
崔璐，杜华强，周国模，李雪建，毛方杰，徐小军，范渭亮，李阳光，朱迪恩，刘腾艳，邢璐琪 (166)

- ### 快报
- 多源数据的嫦娥四号着陆点定位
邱凯昌，刘召芹，刘斌，万文辉，彭漫，王晔昕，苟盛，岳宗玉，辛鑫，贾萌娜，牛胜利 (181)

JOURNAL OF REMOTE SENSING

(Vol. 23 No.1 January , 2019)

CONTENTS

Review

- Geometric-optical remote sensing modeling to quantitative remote sensing theory and methodology development:
In memory of academician Li Xiaowen
..... *LIU Qinhua, YAN Guangjian, JIAO Ziti, XIAO Qing, WEN Jianguang, LIANG Shunlin, WANG Jindi* (10)

Fundamental Research

- Advances and challenges in the validation of remote sensing albedo products
..... *WU Xiaodan, XIAO Qing, WEN Jianguang, YOU Dongqin* (23)
The progress introduction on the study of surface net radiation flux observation, simulation, and assimilation
..... *ZHAO Lifang, SHEN Zhanfeng, LI Chunming, GAO Lijing, GUO Ming, SUN Yuan, PENG Man* (36)
Retrieval of sun-induced chlorophyll fluorescence and advancements in carbon cycle application
..... *ZHANG Zhaoying, WANG Songhan, QIU Bo, SONG Lian, ZHANG Yongguang* (52)
Preliminary verification of Landsat satellite albedo from airborne WIDAS data
..... *HE Dandan, JIAO Ziti, DONG Yadong, ZHANG Xiaoning, DING Anxin, YIN Siyang, CUI Lei, CHANG Yaxuan* (61)
Retrieval of fuel moisture content by using radiative transfer models from optical remote sensing data
..... *QUAN Xingwen, HE Binbin, LIU Xiangzhuo, LIAO Zhanmang, QIU Shi, YIN Changming* (77)

Technology and Methodology

- InSAR interference phase filtering based on joint EEMD-KECA algorithm
..... *YU Jie, LIU Limin, LI Xiaojuan, ZHU Lin, XIE Donghai, CHEN Mi* (88)
Full-waveform LiDAR echo decomposition method *LI Hongpeng, LI Guoyuan, CAI Zhijian, WU Guanhao* (98)
Effect of sinusoidal phase-modulated scatter-wave jamming to the jamming suppression of SAR dual-channel cancellation *ZHANG Yunpeng, BI Daping, ZHOU Yang, ZHANG Bo, FANG Mingxing* (107)
Detecting atmospheric-water optical property profiles with a polarized lidar
..... *ZHOU Yudi, LIU Dong, XU Peituo, MAO Zhihua, CHEN Peng, LIU Zhipeng, LIU Qun, TANG Peijun, ZHANG Yupeng, WANG Xueji, REN Jiawei, JIN Shiwei* (115)
Analysis on the radiation effects of a charge-coupled device in a space debris detection satellite in orbit
..... *LI Yudong, WEN Lin, HUANG Jianyu, WEN Yan, ZHANG Keke, GUO Qi* (124)

Remote Sensing Applications

- Study on hierarchical building extraction from high resolution remote sensing imagery
..... *YOU Yongfa, WANG Siyuan, WANG Bin, MA Yuanxu, SHEN Ming, LIU Weihua, XIAO Lin* (135)
Comparative analysis of long-term (2005—2016) spatiotemporal variations in high-level tropospheric formaldehyde (HCHO) in Guangdong and Jiangsu Provinces in China
..... *ZHU Songyan, LI Xiaoying, CHENG Tianhai, YU Chao, WANG Xinhui, MIAO Jing, HOU Can* (153)
Spatial patterns and correlations in the richness of bird and mammal species and environmental factors in Xinjiang, China *LONG Changyu, WAN Huawei, LI Liping, WANG Jindi* (165)
Combination of decision tree and mixed pixel decomposition for extracting bamboo forest information in China ...
..... *CUI Lu, DU Huaqiang, ZHOU Guomo, LI Xuejian, MAO Fangjie, XU Xiaojun, FAN Weiliang, LI Yangguang, ZHU Dien, LIU Tengyan, XING Luqi* (176)

Progress

- Chang'e-4 lander localization based on multi-source data
..... *DI Kaichang, LIU Zhaoqin, LIU Bin, WAN Wenhui, PENG Man, WANG Yexin, GOU Sheng, YUE Zongyu, XIN Xin, JIA Mengna, NIU Shengli* (177)

Chang'e-4 lander localization based on multi-source data

DI Kaichang, LIU Zhaoqin, LIU Bin, WAN Wenhui, PENG Man, WANG Yexin, GOU Sheng,
YUE Zongyu, XIN Xin, JIA Mengna, NIU Shengli

*State Key Laboratory of Remote Sensing Science, Institute of Remote Sensing and Digital Earth, Chinese Academy of Sciences,
Beijing 100101, China*

Abstract: High precision localization of Chang'e-4 lander is critical to support safe and efficient mission operations. This paper presents the lander localization techniques, including image feature matching and monoscopic image measurement, using digital orthophoto maps of Chang'e-2 and LROC NAC images, descent camera images and monitoring camera image of Chang'e-4 lander. The lander location is precisely determined to be (177.588°E, 45.457°S) using these techniques. Localization of the lander in multiple datasets is valuable for synergistic scientific investigation of the landing site.

Key words: Chang'e-4, lander localization, descent camera image, monitoring camera image, multi-source data

Citation formate: Di K C, Liu Z Q, Liu B, Wan W H, Peng M, Wang Y X, Gou S, Yue Z Y, Xin X, Jia M N and Niu S L. 2019. Chang'e-4 lander localization based on multi-source data. Journal of Remote Sensing, 23(1): 177–184 [DOI:[10.11834/jrs.2019015](https://doi.org/10.11834/jrs.2019015)]

Chang'e-4 (CE-4) is one of the key missions in the Chinese Lunar Exploration Program (Jia et al., 2018). With the support of the Queqiao (Magpie Bridge) relay satellite, CE-4 lunar probe has successfully landed on the far side of the moon in Von Kármán crater inside the South Pole-Aitken (SPA) basin at 10:26 am on January 3, 2019. The rover was successfully released from the lander and touched on the lunar surface on the same day. The success of this task marked the first soft landing of human spacecraft on the far side of the moon, which opened a new era of lunar exploration.

CE-4 lander localization is a fundamental work to support mission operations and science applications. High precision lander localization is of great significance for mission planning and safe and efficient implementation of the plans (Jia et al., 2014; Wan et al., 2014; Liu et al., 2015). In addition, determination of lander location in multiple datasets is particularly important for synergistic use of these datasets in scientific investigation of the landing site.

In the CE-4 mission operations, the Planetary Remote Sensing team of State Key Laboratory of Remote Sensing Science has been participating in the teleoperation tasks in Beijing Aerospace Control Center. Based on digital orthophoto maps (DOMs) generated from multiple orbital images, descending images from the lander's descent camera, and the ground image from the lander's monitoring camera, we have determined the lander location with high precision, using techniques of image feature matching, monoscopic image measurement, etc. The lander localization result has been used to support mission operations. In this short article, we briefly present the lander localization techniques and the results.

1 DATA

The high-resolution DOMs generated from orbital images are used as the reference maps for CE-4 lander localization. At present, Chang'e-2 (CE-2) orbital image data is the highest-resolution stereo

Received: 2019-01-06; **Version of record first published:** 2019-01-09

Foundation: The Key Research Program of the Chinese Academy of Sciences (No. XDPB11); National Natural Science Foundation of China (No. 41671458, 41771488)

First author biography: DI Kaichang (1967—), male, professor. His research interests are planetary remote sensing and mapping, navigation and localization. E-mail: dikc@radi.ac.cn

Corresponding author biography: LIU Zhaoqin (1973—), male, associate professor. His research interests are planetary remote sensing and mapping, navigation and localization. E-mail: liuzq@radi.ac.cn

image data that covers the entire moon surface (Ye et al., 2013). The 7 m resolution DOM and 20 m resolution digital elevation model (DEM) products of the entire moon have been produced and released (Li et al., 2018). The Lunar Reconnaissance Orbiter Camera (LROC) Narrow Angle Camera (NAC) has acquired high resolution (up to 0.5 m) images of nearly the entire moon. Because the LROC NAC is not a stereo imaging camera, it only acquired stereo images by side swing in a very limited number of regions (Robinson et al., 2010). The SLDEM2015 (Barker et al., 2016), generated by integration of a DEM generated by the Japanese Selenological and Engineering Explorer (SELENE) terrain camera and product of Lunar Reconnaissance Orbiter Laser Altimeter (LOLA), was also utilized for terrain analysis and sky visibility analysis.

A downward-looking descent camera identical to that on Chang'e-3 is mounted in the bottom of CE-4. The field of view (FOV) is 45.4° with the image size of 1024×1024 pixels (Liu et al., 2015; Wan et al., 2014; Liu et al., 2014). The camera took a series of images during the descending process. However, because of the limitation of the communication bandwidth, the strategies of selective sampling and image compression with a ratio of 1 : 64 were used when transferring the descent images for quick view.

Three monitoring cameras, which have the image size of 1024×1024 pixels and 60° FOV, are mounted on the lander of CE-4. Monitoring cameras A and B

are on the top of the lander, and monitor camera C is on the front panel of the lander with pitch angle of 15° and height of 1.42 m. Monitoring camera C can surveille the front view of the lander, which provides important information for safe separation of the rover from the lander.

2 LANDER LOCALIZATION TECHNIQUES AND RESULTS

A rough location of the lander is first determined by matching a medium resolution (similar to that of the orbital DOM) descent camera image to the orbital DOM. Next, the lander location is transferred to other descent images by sequential image matching. Finally, the lander location is refined by combining the monoscopic measurements from the monitoring camera image (Wan et al., 2014; Liu et al., 2015).

Because the descent images have been heavily compressed and even have some mosaic effects, these images have been pre-processed with the parabolic model to enhance the image quality and consequently to improve the image matching accuracy. For comparison purpose, the descent images are matched to both CE-2 and LROC NAC DOMs. Figure 1 shows the image matching results, the middle image is a descent image taken at about 4 km altitude, the left and right images are the CE-2 and LROC NAC DOMs respectively. The labels A, B and C are the matched corresponding craters for lander localization.

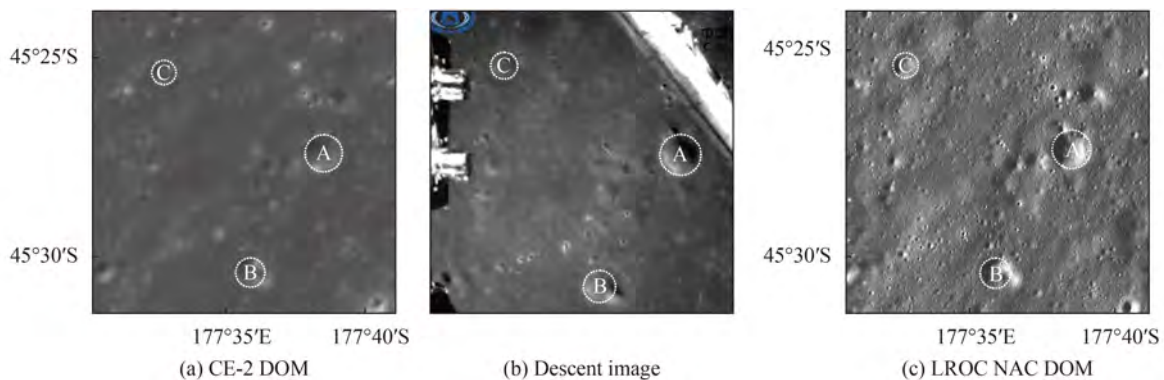


Fig. 1 Feature matching results of multiple data

During the mission, monoscopic measurement technique was applied to monitoring camera C

(referred as the monitoring camera) in order to accomplish a series of tasks, including distance

measurement from the lander, obstacle size measurement, and calculations of the illumination and communication occlusion envelopes. These measurements supported the decision making for rover-lander separation and high precision lander localization. More specifically, under the assumption that the front of the landing point is a horizontal plane, with monitoring camera image coordinates, its object space coordinates in the lander local coordinate system can be calculated according to the lander position and orientation and the camera installation matrix. Then the sizes of the rocks and impact craters as well as their distances to the lander can be calculated (Zhao et al., 2014). Based on the same method, the illumination and communication occlusion envelopes can be calculated according to the azimuth and elevation angles of the sun and the relay satellite, in order to avoid that the rover enters the lander-induced shadow or blind zone of communication when the rover is separated from the lander. Figure 2 shows the monoscopic measurement results of the monitoring camera image, in which the white lines indicate the distances to the front panel of the lander, and the diameter of the front crater is about 29 m.

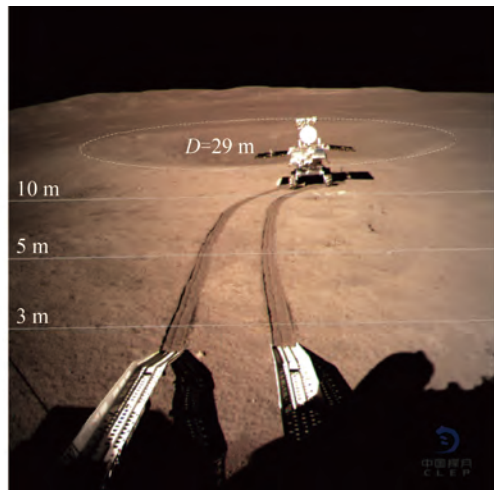


Fig. 2 Monoscopic measurement results of the monitoring camera image(The white lines indicate the distances to the front panel of the lander, and the diameter of the crater is about 29 m)

Finally, the lander location was refined by combining the measurement results from the monitoring camera image and high resolution descent images. The lander location was precisely determined to be (177.588°E , 45.457°S) on the LROC NAC DOM. Meanwhile, the lander location was also determined on CE-2 DOM and SLDEM2015. Figure 3 shows the CE-4 lander localization maps based on LROC NAC DOM, in which the right map is the zoom-in view of the rectangle in the left map.

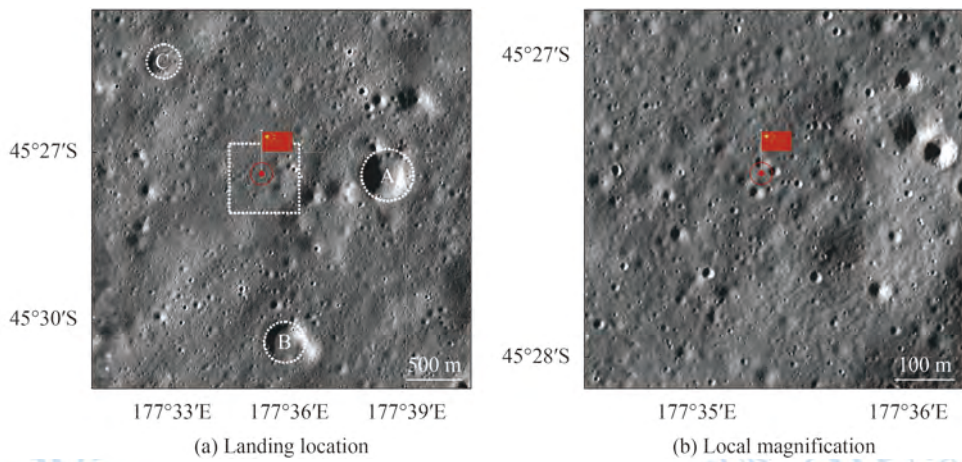


Fig. 3 CE-4 lander localization result on LROC NAC DOM

3 CONCLUSION

This paper presented the techniques of CE-4 lander localization using orbital basemaps, descent images and monitoring camera image. The lander

location was determined to be (177.588°E , 45.457°S) on the LROC NAC DOM. Meanwhile, the lander location was also determined on CE-2 DOM and SLDEM2015. High precision lander localization in multi-source data is valuable to support mission

operations and synergistic scientific investigation of the landing site.

Acknowledgements: The authors gratefully acknowledge Beijing Aerospace Control Center for their support to this study. The authors also thank the institutions/organizations for making the data used in this paper available. The original images of Fig. 1(b) and Fig. 2 were downloaded from the website of China's Lunar and Deep Space Exploration (<http://www.clep.org.cn>), thank you all here.

REFERENCES

- Barker M K, Mazarico E, Neumann G A, Zuber M T, Haruyama J, Smith D E. 2016. A new lunar digital elevation model from the Lunar Orbiter Laser Altimeter and SELENE Terrain Camera. *Icarus*, 273: 346–355 [DOI: [10.1016/j.icarus.2015.07.039](https://doi.org/10.1016/j.icarus.2015.07.039)]
- Jia Y, Liu S, Li M, Li Q, Peng S, Wen B, Ma Y and Zhang S. 2014. Chang'E-3 system pinpoint landing localization based on descent image sequence. *Chinese Science Bulletin*, 59(19): 1838–1843 [DOI: [10.1360/N972014-00020](https://doi.org/10.1360/N972014-00020)]
- Jia Y, Zou Y, Xue C, Ping J, Yan J and Ning Y. 2018. Scientific objectives and payloads of Chang'E-4 mission. *Chinese Journal of Space Science*, 38(1): 118–130 [DOI: [10.11728/cjss2018.01.118](https://doi.org/10.11728/cjss2018.01.118)]
- Li C, Liu J, Ren X, Yan W, Zuo W, Lingli M, Zhang H, Yan S, Wen W, Tan X, Xiaoxia Z, Wenrui W, Qiang F, Liang G, Guangliang Z, Baochang Z, Jianfeng Y and Ouyang Z. 2018. Lunar Global High-precision Terrain Reconstruction Based on Chang'e-2 Stereo Images. *Geomatics and Information Science of Wuhan University*, 43(4): 485–495 [DOI: [10.13203/j.whugis20170400](https://doi.org/10.13203/j.whugis20170400)]
- Liu Z, Di K, Peng M, Wan W, Liu B, Li L, Yu T, Wang B, Zhou J, Chen H. 2015. High precision landing site mapping and rover localization for Chang'e-3 mission. *Science China-physics Mechanics & Astronomy*, 58(1): 1–11
- Robinson M S, Brylow S M, Tschimmel M, Humm D C, Lawrence S J, Thomas P C, Denevi B W, Bowmansneros E, Zerr J, Ravine M A. 2010. Lunar Reconnaissance Orbiter Camera (LROC) Instrument Overview. *Space Science Reviews*, 150: 81–124 [DOI: [10.1007/s11214-010-9634-2](https://doi.org/10.1007/s11214-010-9634-2)]
- Wan W, Liu Z, Liu Y, Liu B, Di K, Zhou J, Wang B, Liu C and Wang J. 2014. Descent Image Matching Based Position Evaluation for Chang'e-3 Landing Point. *Spacecraft Engineering*, 23(4): 5–12
- Ye P, Huang J, Zhang Y and Meng L. 2013. Technological achievements of Chang'E-2 probe and prospect of deep space exploration in China. *Science China: Technical Science*, 7: 467–477 [DOI: [10.1360/092013-229](https://doi.org/10.1360/092013-229)]
- Zhao Q, Liu Z, Wan W, Li W, Sun Y, Di K, Zhou J, Xi L and Tie W. 2014. Decision support for separation of Chang'e-3 rover and lander based on monoscopic measurement using monitoring camera image. *Journal of Remote Sensing*, 18(5): 981–987 [DOI: [10.11834/jrs.20144070](https://doi.org/10.11834/jrs.20144070)]

多源数据的嫦娥四号着陆点定位

邸凯昌, 刘召芹, 刘斌, 万文辉, 彭嫚, 王晔昕, 范盛, 岳宗玉,
辛鑫, 贾萌娜, 牛胜利

中国科学院遥感与数字地球研究所 遥感科学国家重点实验室, 北京 100101

摘要: 嫦娥四号着陆点的精确定位对于工程任务安全高效实施至关重要。本文基于嫦娥二号正射影像、LROC NAC正射影像、嫦娥四号降落相机影像、嫦娥四号监视相机影像等多源数据, 利用影像特征匹配定位和单像视觉测量定位技术, 确定了嫦娥四号着陆点的精确位置为(177.588°E, 45.457°S)。本研究结果对综合利用多源数据深入开展着陆区科学的研究具有重要意义。

关键词: 嫦娥四号, 着陆点定位, 降落相机影像, 监视相机影像, 多源数据

引用格式: 邸凯昌, 刘召芹, 刘斌, 万文辉, 彭嫚, 王晔昕, 范盛, 岳宗玉, 辛鑫, 贾萌娜, 牛胜利. 2019. 多源数据的嫦娥四号着陆点定位. *遥感学报*, 23(1): 177–184

Di K C, Liu Z Q, Liu B, Wan W H, Peng M, Wang Y X, Gou S, Yue Z Y, Xin X, Jia M N and Niu S L. 2019. Chang'e-4 lander localization based on multi-source data. *Journal of Remote Sensing*, 23(1): 177–184
[DOI:[10.11834/jrs.20199015](https://doi.org/10.11834/jrs.20199015)]

嫦娥四号(CE-4)是中国月球探测工程的一项重要任务(贾瑛卓等, 2018)。在“鹊桥”中继星的支持下, 嫦娥四号探测器已于2019-01-03 10:26在月球背面预选着陆区南极-艾特肯盆地(South Pole-Aitken basin)内的冯·卡门撞击坑成功软着陆, 并于当日成功实现两器分离, 这是人类探测器首次在月球背面软着陆, 开启了人类月球探测新篇章。

CE-4着陆点定位是支持工程任务实施和科学应用研究的基础性工作。着陆点的高精度定位对于后续巡视探测工程任务的规划和安全高效实施至关重要(贾阳等, 2014; 万文辉等, 2014; Liu等, 2015)。目前, 国内外多个探测任务已经获取了着陆区的多种遥感数据, 在这些多源月球遥感数据中同时确定着陆点位置, 不仅可实现着陆点的高精度定位, 而且有利于综合利用多源数据对着陆区开展深入的科学的研究。

在CE-4工程任务中, 遥感科学国家重点实验室行星遥感团队在北京航天飞行控制中心参加了

遥操作任务, 基于多源轨道器影像底图、CE-4着陆器降落相机序列影像、着陆器监视影像等, 利用影像特征匹配定位、单像视觉测量定位等技术, 确定了着陆点的精确位置, 支持了工程任务。本文简要介绍着陆点定位技术和CE-4着陆点定位结果。

1 数 据

月球表面大范围、高分辨率的轨道器影像产品是着陆器定位的基准底图, 目前覆盖全月的最高分辨率立体影像数据为嫦娥二号(CE-2)轨道器影像(叶培建等, 2013), 现已制成并发布了全月的7 m分辨率正射影像(DOM)及20 m分辨率的数字高程模型(DEM)产品(李春来等, 2018)。月球勘测轨道器相机LROC(Lunar Reconnaissance Orbiter Camera)的窄角相机NAC(Narrow Angle Camera)获取了几乎全月表高分辨率影像, 其最高分辨率可达0.5 m, LROC NAC不是立体成像相机, 所以只

收稿日期: 2019-01-06; 预印本: 2019-01-09

基金项目: 中国科学院B类先导科技专项培育项目(编号: XDPB11); 国家自然科学基金(编号: 41671458, 41771488)

第一作者简介: 邸凯昌, 1967年生, 男, 研究员。研究方向为行星遥感制图与导航定位。E-mail: dike@radi.ac.cn

通信作者简介: 刘召芹, 1973年生, 男, 副研究员, 研究方向为行星遥感制图与导航定位。E-mail: liuzq@radi.ac.cn

在少数区域通过相机侧摆获取立体像对(Robinson等, 2010)。本文以CE-2制作的DOM和LROC NAC影像制作的高分辨率DOM作为基准底图, 同时还利用了由“月亮女神”(SELENE)搭载的地形测绘相机与月球激光高度计(LOLA)融合生成的SLDEM2015(Barker等, 2016)进行了地形分析、天际线计算等。

CE-4着陆器底部以向下垂直视角安置了同嫦娥三号相同的降落相机。降落相机像幅为1024像素×1024像素, 视场角为45.4°(Liu等, 2015; 万文辉等, 2014; 刘斌等, 2014), 在着陆过程中获取了分辨率由低到高的序列降落影像。由于“鹊桥”中继星数据链路带宽有限, 因而降落时以抽帧方式下传多张1:64压缩的降落影像, 这些数据用于与轨道器基准底图的匹配定位。

CE-4着陆器上安置了3台监视相机, 像幅为1024像素×1024像素, 视场角为60°。其中, 监视相机A、B安装于着陆器顶部, 监视相机C以15°俯仰角安装于着陆器前面板1.42 m高处, 用于监视着陆

器正前方视场, 为两器分离决策提供支持(赵强等, 2014)。

2 定位方法与结果

着陆点的定位首先通过中分辨率降落相机影像(与轨道器影像分辨率相当)与轨道器DOM的特征匹配, 获得初始定位结果, 进一步通过序列降落影像的匹配, 实现着陆点位置的传递。最后通过监视相机影像的量测结果, 精化着陆点的定位结果(万文辉等, 2014; Liu等, 2015)。

由于着陆过程中实时下传的高压缩比降落图像马赛克效应严重, 因而匹配定位处理之前引入抛物线模型进行影像预处理, 提升降落影像质量, 进而提升降落影像与轨道器DOM的匹配精度。为了对比验证, 将降落相机影像同时匹配到CE-2和LROC NAC影像底图。图1是匹配定位结果, 其中图1(b)是4 km高度拍摄的降落影像, 图1(a)和图1(c)分别是CE-2和LROC NAC DOM, 标识A、B、C为识别出的用于定位的同名撞击坑。

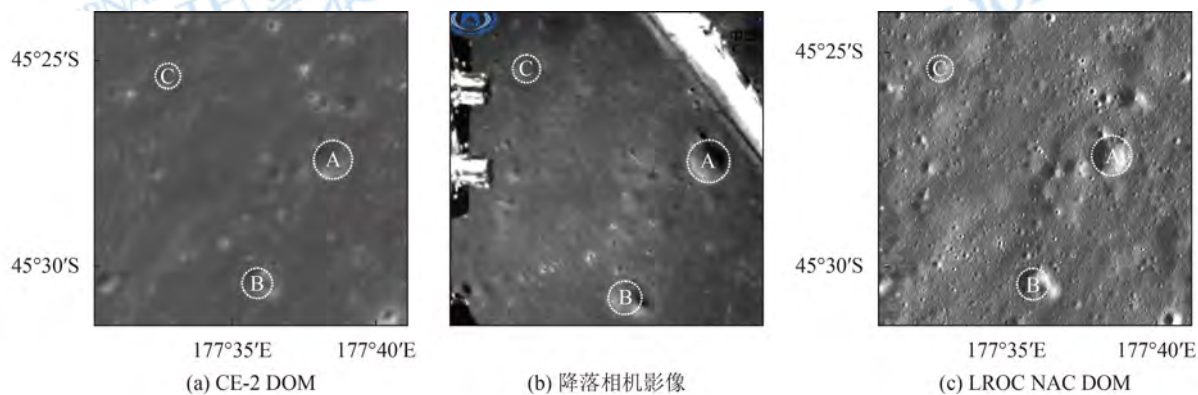


图1 多源数据特征匹配结果

工程中基于单像量测技术, 利用监视相机C(下称监视相机)完成了着陆器前方距离和障碍物量测、光照及通信遮挡包络计算等任务, 有效支持了两器分离决策及着陆点精确定位。监视相机单像量测技术是假设着陆点前方为一水平面, 从监视相机像平面坐标, 根据着陆器姿态及相机安装位置计算该点对应的着陆器月面局部坐标系下的物方坐标, 进而确定两器分离任务区域内石块和撞击坑大小及与着陆器的相对距离(赵强等, 2014)。利用同样方法根据太阳及中继星的方位角和高度角计算光照和通信遮挡, 避免在两器分离

时巡视器停留在阴影或通信盲区。图2展示了监视相机单像量测结果, 白色横线表示到着陆器前面板的距离, 前方撞击坑直径约为29 m。

最后, 基于监视相机影像量测结果, 结合降落相机高分辨率影像对着陆点位置进行精化, 得到着陆点在LROC NAC基准底图上的精确位置为(177.588°E, 45.457°S)。同时, 在嫦娥二号DOM和SLDEM2015中也确定了着陆点的精确位置。图3为以LROC NAC底图为基准的嫦娥四号着陆点定位图, 其中图3(b)是图3(a)方框中的局部放大图。

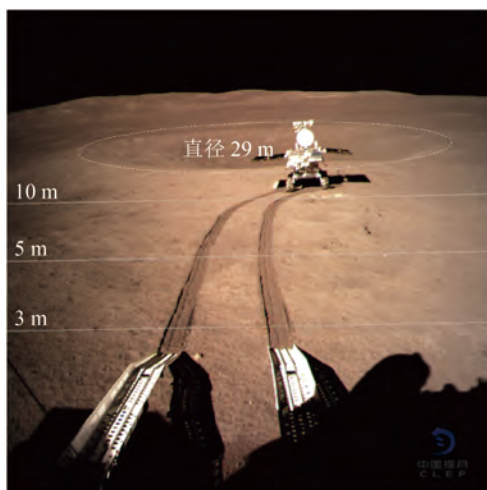
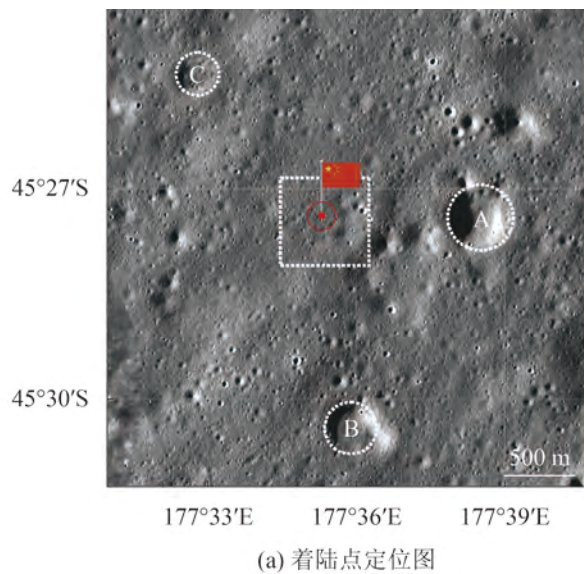
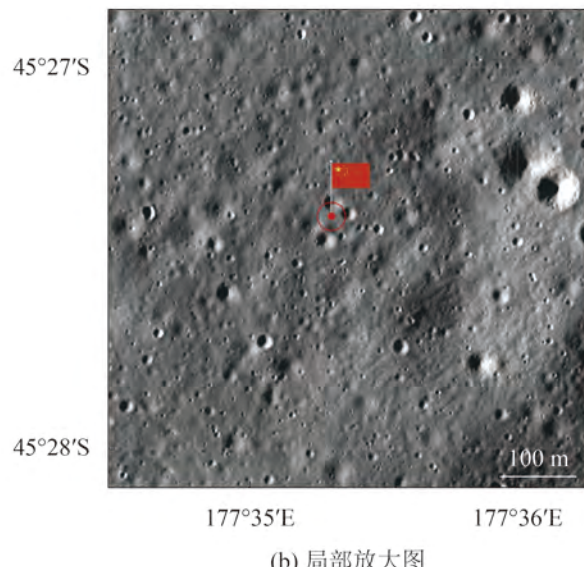


图2 监视相机单像量测结果(白线表示到着陆器前板的距离,撞击坑直径约为29 m)



(a) 着陆点定位图



(b) 局部放大图

图3 以LROC NAC底图为基准的嫦娥四号着陆点定位图

3 结 论

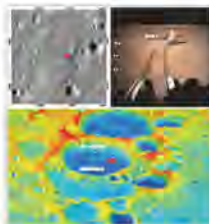
本文简要介绍了CE-4着陆点定位方法和结果,利用轨道器影像底图、着陆器降落相机影像、着陆器监视相机影像,通过影像匹配和视觉测量定位技术,确定了着陆点的位置,着陆点在LROC NAC基准底图上的精确位置为(177.588° E, 45.457° S)。同时,着陆点位置也精确地定位到CE-2 DOM及SLDEM2015中。CE-4着陆点的精确定位,支持了工程任务的实施,也有助于综合利用多源数据开展着陆区科学的研究。

志 谢 衷心感谢北京航天飞行控制中心对本研究的支持,并感谢本研究中所用数据的生产和发布单位!文中图1(b)和图2原始图像来源于中国探月与深空探测网 (<http://www.clep.org.cn>) ,在此一并感谢!

参考文献(References)

- Barker M K, Mazarico E, Neumann G A, Zuber M T, Haruyama J, Smith D E. 2016. A new lunar digital elevation model from the Lunar Orbiter Laser Altimeter and SELENE Terrain Camera. *Icarus*, 273: 346–355 [DOI: [10.1016/j.icarus.2015.07.039](https://doi.org/10.1016/j.icarus.2015.07.039)]
- Jia Y, Liu S, Li M, Li Q, Peng S, Wen B, Ma Y and Zhang S. 2014. Chang'E-3 system pinpoint landing localization based on descent image sequence. *Chinese Science Bulletin*, 59(19): 1838–1843 (贾阳, 刘少创, 李明磊, 李群智, 彭松, 温博, 马友青, 张烁. 2014. 利用降落影像序列实现嫦娥三号系统着陆点高精度定位. *科学通报*, 59(19): 1838–1843) [DOI: [10.1360/N972014-00020](https://doi.org/10.1360/N972014-00020)]
- Jia Y, Zou Y, Xue C, Ping J, Yan J and Ning Y. 2018. Scientific objectives and payloads of Chang'E-4 mission. *Chinese Journal of Space Science*, 38(1): 118–130 (贾瑛卓, 邹永廖, 薛长斌, 平劲松, 严俊, 宁远明. 2018. 嫦娥四号任务科学目标和有效载荷配置. *空间科学学报*, 38(1): 118–130) [DOI: [10.11728/cjss2018.01.118](https://doi.org/10.11728/cjss2018.01.118)]
- Li C, Liu J, Ren X, Yan W, Zuo W, Lingli M, Zhang H, Yan S, Wen W, Tan X, Xiaoxia Z, Wenrui W, Qiang F, Liang G, Guangliang Z, Baochang Z, Jianfeng Y and Ouyang Z. 2018. Lunar Global High-precision Terrain Reconstruction Based on Chang'e-2 Stereo Images. *Geomatics and Information Science of Wuhan University*, 43(4): 485–495 (李春来, 刘建军, 任鑫, 严伟, 左维, 牟伶俐, 张洪波, 苏彦, 温卫斌, 谭旭, 张晓霞, 王文睿, 付强, 耿良, 张广良, 赵葆常, 杨建峰, 欧阳自远. 2018. 基于嫦娥二号立体影像的全月高精度地形重建. *武汉大学学报·信息科学版*, 43(4): 485–495) [DOI: [10.13203/j.whugis20170400](https://doi.org/10.13203/j.whugis20170400)]

- Liu Z, Di K, Peng M, Wan W, Liu B, Li L, Yu T, Wang B, Zhou J, Chen H. 2015. High precision landing site mapping and rover localization for Chang'e-3 mission. *Science China-Physics Mechanics & Astronomy*, 58(1): 1–11
- Robinson M S, Brylow S M, Tschimmel M, Humm D C, Lawrence S J, Thomas P C, Denevi B W, Bowmansneros E, Zerr J, Ravine M A. 2010. Lunar Reconnaissance Orbiter Camera (LROC) Instrument Overview. *Space Science Reviews*, 150: 81–124 [DOI: [10.1007/s11214-010-9634-2](https://doi.org/10.1007/s11214-010-9634-2)]
- Wan W , Liu Z, Liu Y, Liu B, Di K, Zhou J, Wang B, Liu C and Wang J. 2014. Descent Image Matching Based Position Evaluation for Chang'e-3 Landing Point. *Spacecraft Engineering*, 23(4): 5–12 (万文辉, 刘召芹, 刘一良, 刘斌, 邱凯昌, 周建亮, 王保丰, 刘传凯, 王稼. 2014. 基于降落图像匹配的嫦娥三号着陆点位置评估. 航天器工程, 23(4): 5–12) [DOI: [10.3969/j.issn.1673-8748.2014.01.002](https://doi.org/10.3969/j.issn.1673-8748.2014.01.002)]
- Ye P, Huang J, Zhang Y and Meng L. 2013. Technological achievements of Chang'E-2 probe and prospect of deep space exploration in China. *Science China: Technical Science*, 7: 467–477 (叶培建, 黄江川, 张廷新, 孟林智. 2013. 嫦娥二号卫星技术成就与中国深空探测展望. 中国科学: 技术科学, 7: 467–477) [DOI: [10.1360/092013-229](https://doi.org/10.1360/092013-229)]
- Zhao Q, liu Z, Wan W, Li W, Sun Y, Di K, Zhou J, Xi L and Tie W. 2014. Decision support for separation of Chang'e-3 rover and lander based on monoscopic measurement using monitoring camera image. *Journal of Remote Sensing*, 18(5): 981–987 (赵强, 刘召芹, 万文辉, 李巍, 孙义威, 邱凯昌, 周建亮, 席露华, 铁伟涛. 2014. 基于监视相机单像量测的嫦娥三号巡视器与着陆器分离决策支持. 遥感学报, 18(5): 981–987) [DOI: [10.11834/jrs.20144070](https://doi.org/10.11834/jrs.20144070)]



封面说明

About the Cover

嫦娥四号着陆点高精度定位图

Chang'e-4 lander high precision localization

嫦娥四号探测器于2019年1月3日在月球背面南极-艾特肯盆地内的冯·卡门撞击坑成功软着陆。封面展示了着陆区数字高程模型(下图)、着陆器监视相机影像单像量测结果(右上图)和嫦娥四号着陆点定位图(左上图)。基于多源影像,利用影像特征匹配定位和单像视觉测量定位技术,确定了嫦娥四号着陆点的精确位置为(177.588°E, 45.457°S)。更多信息及技术细节见本期177页。

Chang'e-4 lunar probe has successfully landed on the far side of the moon in Von Kármán crater inside the South Pole-Aitken (SPA) basin on January 3, 2019. The front cover shows the digital elevation model of the landing site (the lower map), the monoscopic measurement results from the monitoring camera image (the upper right map), and the lander localization map (the upper left map). The lander location was precisely determined to be (177.588° E, 45.457° S) based on multi-source data using image feature matching and monoscopic image measurement techniques. More information and technical details can be found in page 177.

遥感学报

JOURNAL OF REMOTE SENSING

YAOGAN XUEBAO (双月刊 1997年创刊)

第23卷 第1期 2019年1月25日

(Bimonthly, Published since 1997)

Vol.23 No.1 January 25, 2019

主 管	中国科学院	Superintended by	Chinese Academy of Sciences
主 办	中国科学院遥感与数字地球研究所 中国地理学会环境遥感分会	Sponsored by	Institute of Remote Sensing and Digital Earth,CAS The Associate on Environment Remote Sensing of China
主 编	顾行发	Editor in Chief	GU Xingfa
编 辑	《遥感学报》编委会 北京市海淀区北四环西路19号 邮编:100190 电话:86-10-58887052 http://www.jors.cn E-mail: jrs@radi.ac.cn	Edited by	Editorial Board of Journal of Remote Sensing Add: P.O.Box 2702, Beijing 100190, China Tel: 86-10-58887052 http://www.jors.cn E-mail: jrs@radi.ac.cn
出 版 社	科学出版社	Published by	Science Press
印 刷 装 订	北京科信印刷有限公司	Printed by	Beijing Kexin Printing Co. Ltd.
总 发 行	科学出版社 北京东黄城根北街16号 国内邮发代号: 82-324 邮政编码: 100717 电话: 86-10-64017032 淘宝店铺名称: 中科期刊	Distributed by	Science Press Add: 16 Donghuangchenggen North Street, Beijing 100717, China Tel: 86-10-64017032 Taobao: Zhongke Journal
国 外 发 行	中国国际图书贸易总公司 北京399信箱 邮政编码: 100044 国外发行代号: BM 1002	Overseas distributed by	China International Book Trading Corporation Add: P.O.Box 399, Beijing 100044, China

中国标准连续出版物号: ISSN 1007-4619
CN 11-3841/TP

CODEN YXAUAB

eISSN 2095-9494

定价: 70.00元



官网



微博



淘宝



微店

ISSN 1007-4619



9 771007 461194